

# Evaporative spray cooling of plain and microporous coated surfaces

J.H. Kim <sup>a</sup>, S.M. You <sup>a</sup>, Stephen U.S. Choi <sup>b,\*</sup>

<sup>a</sup> *The University of Texas at Arlington, Department of Mechanical and Aerospace Engineering, P.O. Box 19023, Arlington, TX 76019-0023, USA*

<sup>b</sup> *Argonne National Laboratory, Energy Technology Division, 9700 S. Cass Avenue, Argonne, IL 60439, USA*

Received 5 September 2003; received in revised form 30 January 2004

Available online 19 March 2004

## Abstract

Experiments were performed on air and evaporative spray cooling of plain and microporous coated surfaces on flat and cylindrical heaters. Micron-size aluminum particles were used to build the microporous structures on the heated surfaces. To analyze the evaporative cooling, heat transfer curves were obtained in the form of the wall temperature difference versus heat flux. The heat transfer coefficients were also determined as a function of heat flux. Three water flow rates (1.25, 1.75 and 2.40 ml/min) were tested for the flat heater and one rate (3.0 ml/min) for the cylindrical heater, maintaining the air pressure of 7 psig (48 kPa) at the inlet of the nozzle. The effect of different particle sizes in the coating was also tested to optimize the microporous coating technique. Spraying water droplets on the microporous coating surface enhanced the heat removal due to the capillary pumping phenomenon through the microporous cavities connecting each other. The evaporative spray cooling increased the heat transfer coefficient by up to 400% relative to that of the uncoated surface cooled by dry air, and this enhancement was maintained at high heat fluxes by using microporous surfaces.

© 2004 Elsevier Ltd. All rights reserved.

*Keywords:* Evaporative spray cooling; Microporous coating; Heat transfer enhancement; Phase change

## 1. Introduction

Evaporative spray cooling obtained by two-phase fluid flow is an effective and economical method to cool heated objects requiring comparatively high heat flux dissipation ( $\approx$  up to 40 kW/m<sup>2</sup>) for numerous industrial applications. Since spray cooling involves liquid-vapor phase change, the increase of heat transfer is significant compared to single-phase forced convection of air. The heat of vaporization augments heat transfer when the tiny water droplets encounter and evaporate from the heated surface.

Recently, various studies have reported on the effectiveness of spray cooling, and numerical analyses have been conducted to understand the behavior of evaporative cooling. Zhou and Yao [1] developed a group model employing the Lagrangian approach and found important information about droplet diameter effects, droplet trajectories, impact velocities, and the impact angles of spray dynamics with significantly fewer droplet group numbers, resulting in a significant reduction in computational time. Chigier [2] developed a systematic characterization method using laser diffraction to measure particle size, velocity and number density, as well as flux of sprays. Choi and Yao [3] investigated fundamental heat transfer mechanisms of horizontal and vertical impacting sprays. They found that a vertical impacting spray has a higher heat transfer coefficient than a horizontal impacting spray due to the secondary contacts of splattered droplets in the film boiling region.

\* Corresponding author. Tel.: +1-630-252-6439; fax: +1-630-252-5568.

E-mail address: [choi@anl.gov](mailto:choi@anl.gov) (S.U.S. Choi).

### Nomenclature

$h$	heat transfer coefficient [W/m <sup>2</sup> -K]
$k$	thermal conductivity [W/m-K]
$q''$	heat flux [kW/m <sup>2</sup> ]

$\Delta T$	temperature difference between wall and ambient [K]
------------	---

Bernardin and Mudawar [4] developed experimental correlations for the film heat transfer efficiency of water droplets, and they found that surface temperature and droplet diameter/velocity are major parameters in the correlations. Stewart and Hagers [5], using a stainless steel specimen cooled from high to ambient temperature, investigated the heat transfer coefficient from various types of spray. They found that the heat transfer coefficient varied with impact density and surface temperature. They also proposed several factors affecting heat removal by spray cooling, including water temperature, surface condition, and impact orientation. Horacek et al [6] conducted spray cooling experiments to investigate the effects of noncondensable gas and subcooling. They achieved comparatively high heat transfer coefficients.

Spray cooling is similar to boiling heat transfer in that both utilize liquid-to-vapor phase change. Both have been extensively studied for cooling the heated objects that generate high heat flux. Different surface microstructures have been previously developed for the heat transfer involved in liquid-vapor phase change [7]. One of the earliest methods used to improve the surface microstructure is to roughen the surface by using sandpaper or some other abrasives. Surface roughening has been proven to significantly enhance the nucleate boiling heat transfer in water and refrigerants [8–11]. Kurihara and Myers [8] showed that the nucleate boiling enhancement was the result of increased active nucleation-site density.

A relatively new method for surface enhancement is the microporous coating developed by O'Connor and You [12] and further refined by Chang and You [13,14]. The coating technique increases vapor/gas entrapment volume and active nucleation-site density by forming openly connected porous structures with cavities of different sizes. The micro-scale porous surface structures can significantly affect the nucleate boiling heat transfer because of the numerous embryonic bubbles in the unique microporous structures. Chang and You [13] reported that the optimum thickness of the microporous coating is about 50  $\mu\text{m}$ .

The main objective of our study is to experimentally measure the effects of water evaporation and microporous coating on cooling with flat and cylindrical heaters. Furthermore, the effects of water flow rate, coating particle sizes, and coating thickness on cooling performance were investigated. The capillary pumping caused by surface tension within the microporous channels is

believed to help the microporous surface retain more water to vaporize than a plain surface; thus, the heat transfer from liquid-to-vapor phase change is used at high heat fluxes. Based upon this fundamental concept, experiments were conducted to study evaporative cooling with plain and coated surfaces for flat and cylindrical heaters.

## 2. Experimental apparatus and procedure

### 2.1. Test facility

The experimental apparatus is shown in Fig. 1. The apparatus includes a test heater that connects the voltage probe and the power supply. The DC power supply was connected to the heater in series with a precision resistor, which was used to measure the electrical current and obtain the heat flux. An HP 3852A Data Acquisition/Control Unit with HP power supply system rated for 0–50 A and 0–60 V was used for obtaining experimental data. This equipment was interfaced via IEEE-488 cables and was connected to a personal computer. T-type thermocouples that had been calibrated with a precision thermometer measured the surface temperature of the heater.

The test heater was attached on the inside wall of a Pyrex glass vessel, as shown in Fig. 1. In this vessel, a nozzle (airbrush by IWATA) was firmly held by a metal

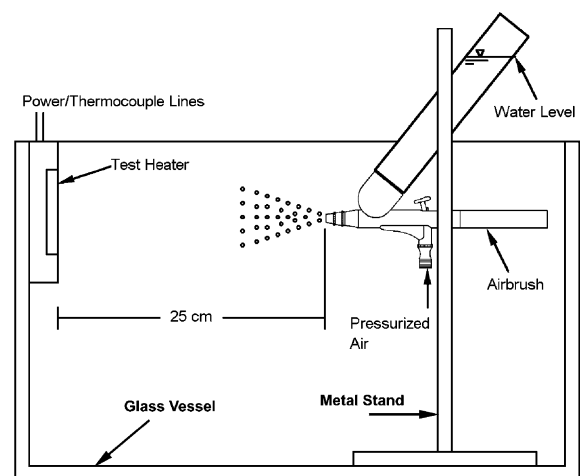


Fig. 1. Schematic view of test section.

stand and was connected to a compressed air source. The spray cone angle was measured as about  $20^\circ$ . For better control of the spray flow rate, a pressure regulator and air filter were used. The water flow rate was maintained at a given value, and the air pressure at the nozzle inlet was set at 7 psig. The 7-psig air pressure was maintained the same throughout all the experiments. The water flow rate was measured by dividing the total volume of water injected through the airbrush by the spray time. The water was at room temperature ( $\approx 22^\circ\text{C}$ ).

## 2.2. Test heaters

The flat surface heater ( $5\text{ cm} \times 5\text{ cm}$ ) used a nichrome wire as a heating element, as shown in Fig. 2 (top). Serpentine windings of the thin nichrome wire (0.144 mm in diameter) are attached to the Teflon substrate (11-mm thick) using Omegabond 200 high-temperature epoxy ( $k \approx 1.4\text{ W/m-K}$ ). A block of copper is bonded on top of the heating element, also using Omegabond 200 epoxy. Two layers of epoxy assure electrical insulation between the copper and the nichrome. To minimize the thickness, the epoxy is cured within an oven maintained at  $150^\circ\text{C}$  while the weight rests on top of the copper

block. Electrical leads are soldered to each end of the nichrome wire. The heating element is set in a Lexan frame and surrounded by a two-part, 3M epoxy (1832L-B/A,  $k \approx 0.067\text{ W/m-K}$ ) to generate a flush-mounted heating surface. The copper block has two holes (1-mm-diameter and 5-mm-depth) drilled into its center from one edge. Two copper-constantan thermocouples (30 gage, 0.255-mm-diameter) are inserted and soldered in the holes to provide surface temperature measurements.

Fig. 2 (bottom) shows a cross section of the large cylindrical test heater. The copper test tube (7.8-cm-long, 1.6-cm-diameter) has three thermocouple holes on each end spaced  $90^\circ$  apart. These 1-mm-diameter holes are 25 mm in length and are drilled axially along the tube. The copper tube is fitted to a commercial cartridge heater (Watlow, Model G3J22, 120 V-500 W), which is 0.95 cm in diameter and 8.9 cm in length (heated length is  $\approx 7.8\text{ cm}$ ). The surface of the cartridge heater is electrochemically plated with a thin copper layer to increase the wettability with molten solder. By heating the copper tube with the cartridge heater, the gap between the components is filled with lead-free silver solder (melting point  $\approx 250^\circ\text{C}$ ). The cartridge heater has a 6-mm-long inactive heating zone at each end. The copper tubes are machined to have the same length as the heated zone of the cartridge heater. The unheated end sections of the cartridge heater are insulated with Teflon blocks and thermally nonconducting epoxy to minimize heat loss.

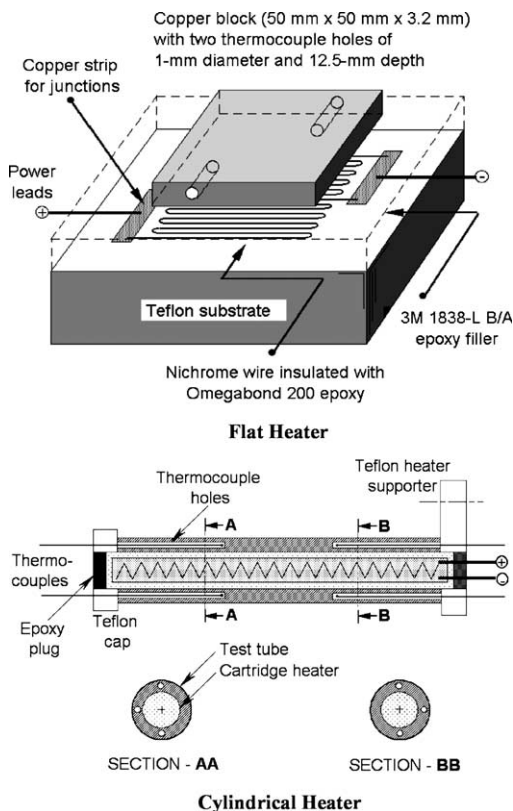


Fig. 2. Schematic view of test heaters (flat and cylindrical).

## 2.3. Uncertainty analysis

Uncertainty for the heat-flux measurement was estimated based upon the values of Chang and You [15], whose heater had the same design but smaller surface size as the present heater. Using the methods of Kline and McClintock [16], heat-flux measurement uncertainty for the present heater was estimated to be smaller than 5%. In addition, temperature measurement uncertainty was estimated by considering the thermocouple calibration error, temperature correction for the embedded thermocouples, and thermocouple resolution error. The uncertainty for the temperature measurement was  $\pm 0.4\text{ K}$ .

## 2.4. Microporous coating technique

The coating material used for the test heater is the ABM introduced by Chang and You [13,14]. The ABM coating was named from the initial letters of its three components: aluminum particles/Devcon brushable ceramic epoxy/methyl-ethyl-ketone (MEK). O'Connor and You [12] developed the microporous coating technique, further refined by Chang and You [13,14] and patented by You and O'Connor [17]. The microporous coating is shown as a scanning electron microscope

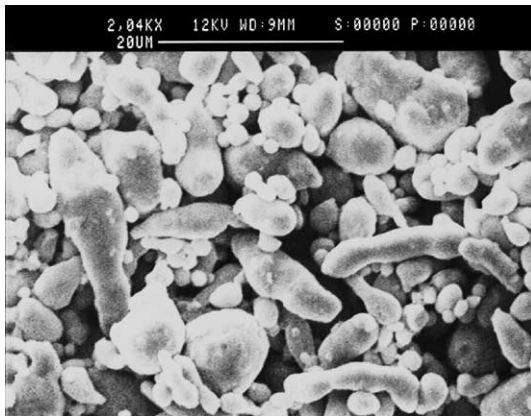


Fig. 3. SEM image of ABM coating.

(SEM) image in Fig. 3. The surface treatment technique increases vapor/gas entrapment volume and active nucleation-site density by forming a porous structure of about 0.1–1  $\mu\text{m}$  size cavities. The ABM mixture was sprayed onto the heater surface using an Iwata HP-C airbrush. After the carrier (MEK) evaporated, the resulting layer consisted of microporous structures with aluminum particles and a binder (Devcon brushable ceramic). The microporous coating provided no significant increase of the heat transfer surface area. The test results of a microporous surface pool boiling in FC-72 revealed significant heat transfer enhancement: (1) boiling incipience occurred five times faster, (2) the nucleate boiling heat transfer coefficient increased by up to 330%, and (3) the critical heat flux increased by 100%.

### 3. Results and discussion

The focus of the present study is to determine the effect of evaporative spray cooling on flat and cylindrical heaters and to extend the evaporative cooling process by application of a microporous coating. Furthermore, we investigated the effects of water flow rate, particle sizes of the coating, and coating thickness on evaporative heat transfer performance. The evaporation curves were in the form of the heat flux versus wall temperature, and the heat transfer coefficient values were compared at the same heat flux to define heat transfer enhancement before “dryout.” The dryout is defined as the state where the liquid–solid contact is very instant so that surface temperature jumps quickly at given heat flux and is similar to the critical heat flux (CHF) in boiling heat transfer. If the wall temperature increases more rapidly (over 30  $^{\circ}\text{C}$  increase for the nominal heat flux increment of 1  $\text{kW}/\text{m}^2$ ) than the previous average wall temperature, it is assumed that dryout has occurred, and power is cut off automatically.

#### 3.1. Dry air-jet cooling-reference case

The dry air-jet cooling tests were performed for plain and microporous surfaces at the same nozzle inlet pressure of 7 psig. For checking of the data, each experiment was performed twice. The microporous structure shown in Fig. 3 enhanced the two-phase heat transfer performance significantly; however, negligible differences between the plain and coated surfaces occurred when an air jet was used to cool the surfaces (Fig. 4). This finding indicates that the increase of area due to the microporous surface structures is negligible for heat transfer by single-phase air convection. The linear correlation for the flat heater is given by

$$q'' = 0.099 \cdot \Delta T \quad (1)$$

The correlation for the cylindrical heater is given by

$$q'' = 0.057 \cdot \Delta T \quad (2)$$

where  $q''$  is the heat flux in  $\text{kW}/\text{m}^2$ , and  $\Delta T$  is the temperature difference between the heated wall and ambient air in  $^{\circ}\text{C}$ . The cooling performance of the cylindrical heater was inferior to that of the flat heater due to the inefficient cooling at the back half of the heater surface. The results from dry air-jet cooling were regarded as a reference case to assess the heat transfer enhancement by evaporative cooling on plain and microporous surfaces.

#### 3.2. Spray cooling results on plain and microporous surfaces

Fig. 5 shows  $q''$  versus  $\Delta T$  for the evaporative spray cooling tests with plain and microporous surfaces; the

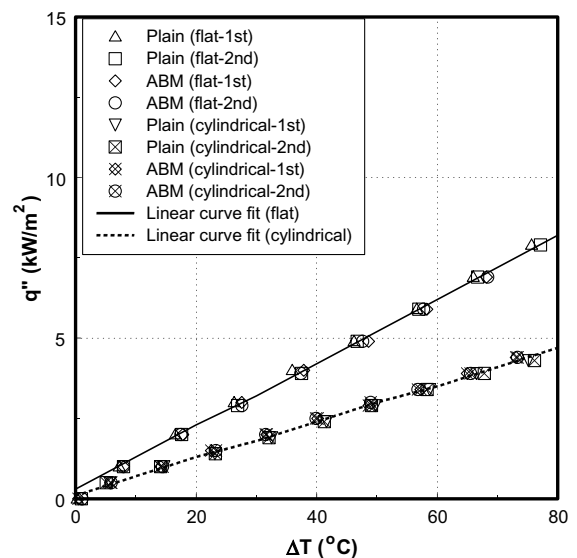


Fig. 4. Heat transfer performance for dry air-jet cooling with flat and cylindrical heaters.

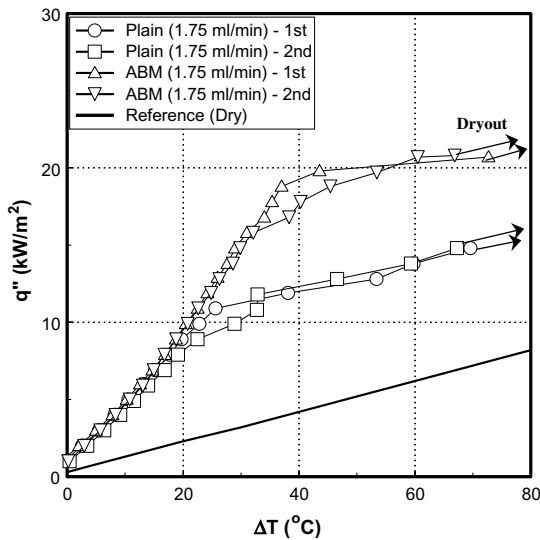


Fig. 5. Heat transfer performance for spray cooling with plain and coated flat heater.

results for dry air-jet cooling are included for comparison. The water flow rate was 1.75 ml/min for both plain and ABM coated surfaces of the flat heater (5 cm × 5 cm). The 8–12 μm size particles were applied to a thickness of ≈50 μm for the ABM coating. As seen in the figure, spraying water droplets on the heated plain surface instead of pure air enhanced the heat transfer rate significantly. For all heat flux values, the improved cooling from having liquid drops in the air jet was obvious. Above 10 kW/m<sup>2</sup> heat flux, however, the enhancement was weaker, showing a parallel increase with the dry air curve. This improved heat transfer occurred mainly because the water droplets evaporate and remove larger amounts of heat from the heater surface. However, above 10 kW/m<sup>2</sup>, a portion of the heater area was dry during the test (“localized dryout”), and this condition resulted in the similar slope with the dry air curve. At about 15 kW/m<sup>2</sup>, the dryout was observed visually, and the wall temperature was rising instantaneously.

As shown in Fig. 5, spray cooling heat transfer was further increased when the microporous coating surface was used instead of the plain surface. In the porous coating, micron-size particles are interconnected, and the connected passages seem to play an important role in the heat transfer performance with evaporative spray cooling. The sprayed water droplets are soaked into the microscale porous structures and spread out to the larger heater area. This behavior is believed to further enhance the heat removal over the plain surface due to the capillary action, by which larger amounts of water are retained for the heated surfaces. Especially at higher heat fluxes (>10 kW/m<sup>2</sup>), the evaporative cooling per-

formance was much better with the ABM coating than the plain surface. The localized dryout point was delayed to higher heat flux (≈18 kW/m<sup>2</sup>), and the cooling performance in the dryout region was also much better. While the dryout occurred at ΔT ≈ 70 °C for the plain surface and ABM coating, the microporous coating extended the dryout heat flux significantly (to ≈21 kW/m<sup>2</sup>).

Fig. 6 compares the heat transfer coefficient versus heat flux for the different surfaces, as well as spray cooling and dry air. When heat flux is less than 10 kW/m<sup>2</sup>, the coated and plain surface show significant increase compared to the dry air case (reference). At this heat flux range, the microporous coating does not provide much additional enhancement over the plain surface. However, at higher heat flux, the coating does provide additional heat transfer. The heat transfer coefficient of the evaporative cooling with the microporous surface was approximately 500 W/m<sup>2</sup>K up to a heat flux of almost 20 kW/m<sup>2</sup>, which is about a 400% increase compared to the reference case. This excellent performance is probably due to the delay of partial dryout.

The cylindrical heater (diameter of 1.6 cm and length of 7.7 cm) was used to investigate the effects of heater surface geometry. The microporous coating had the same size of particles and thickness as the flat heater. The water flow rate of cross-flow spray for the cylindrical heater was approximately 3.0 ml/min, as determined by the ratio of the surface areas of the heaters. Fig. 7 shows the improvement from spray cooling and the microporous coating. The increase was less for the cylindrical heater (≈50% less) than the flat heater due to

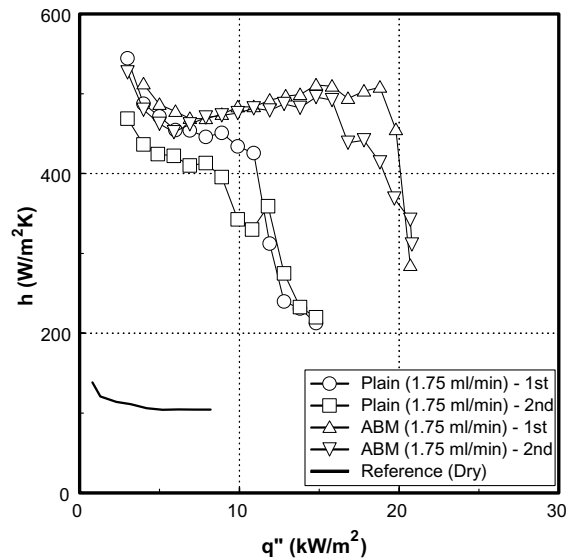


Fig. 6. Heat transfer coefficient versus heat flux for plain and microporous surfaces with flat heater.

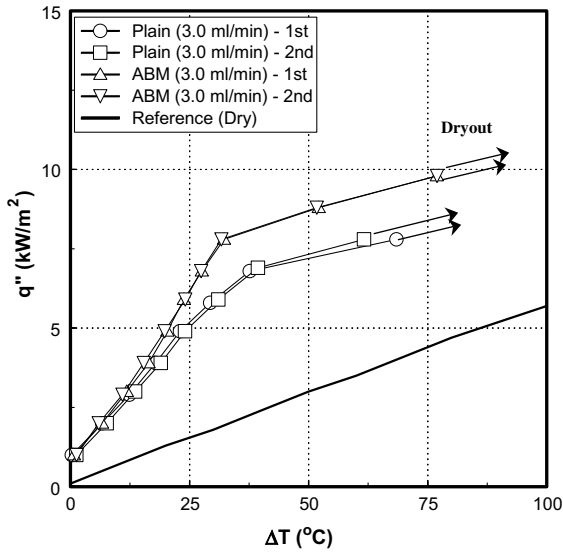


Fig. 7. Heat transfer performance for spray cooling of plain and microporous surfaces with cylindrical heater.

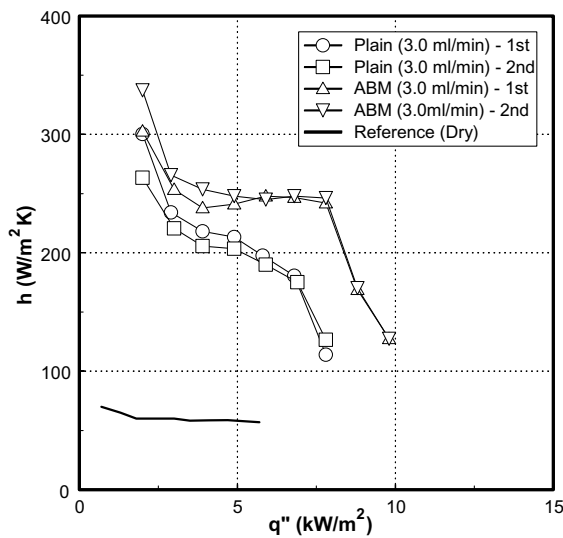


Fig. 8. Heat transfer coefficient versus heat flux for plain and microporous surfaces with cylindrical heater.

the nonwetting surface area in the back surface to the spray. A similar phenomenon occurred in dry air-jet cooling (Fig. 4). Therefore, the heater geometry shows reasonable differences in effects on evaporative heat transfer. If the whole surface is wetted by sprayed water droplets, both flat and cylinder heaters will provide a similar enhancement. The heat transfer coefficient versus heat flux for the cylindrical heater is plotted in Fig. 8. The plain surface showed about 300% increased per-

formance for sprayed water compared to dry air, and additional improvement was found with the microporous surface over the plain surface.

### 3.3. Effects of sprayed water flow rate

Water flow rates of 1.25, 1.75, and 2.4 ml/min were tested to investigate the trends of evaporative spray heat transfer on plain and microporous surfaces of the flat heater. The results are plotted in Fig. 9. Air flow through the nozzle was controlled consistently by maintaining air pressure at the nozzle inlet (7 psig). When heat flux was less than  $\approx 10 \text{ kW/m}^2$ , the flow rates had no effect on the spray cooling curves. However, for higher heat fluxes with spray cooling, the heat transfer increased as the water flow rate increased for both plain and microporous surfaces. This improvement resulted because the available amount of water, fed from the sprayed droplets to be vaporized, increases as the water flow rate increases. For all three flow rates at a given  $\Delta T$ , the microporous structure consistently generated  $\approx 50\%$  enhancement in heat transfer compared to that of the plain surface. For both plain and microporous coated surfaces, the dryout heat flux also increased by about the same amount as the water flow rate was increased.

### 3.4. Microporous coating optimization

We attempted to optimize the microporous structures for evaporative spray heat transfer. The particle sizes and coating thicknesses were investigated as experimental variables. The water flow rate was 1.75 ml/min.

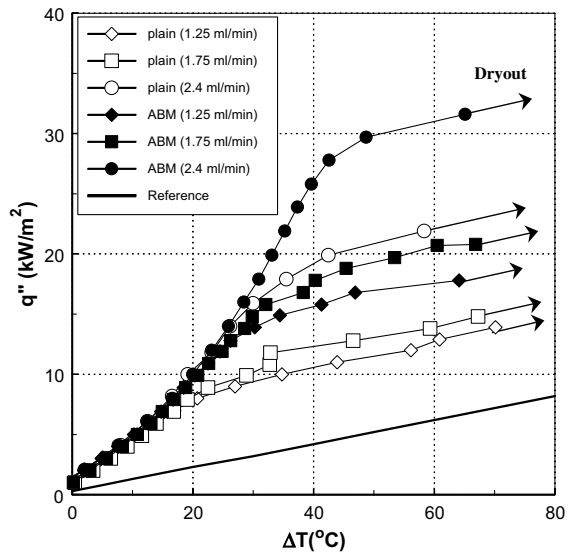


Fig. 9. Effect of water flow rate on heat transfer performance for flat heater.

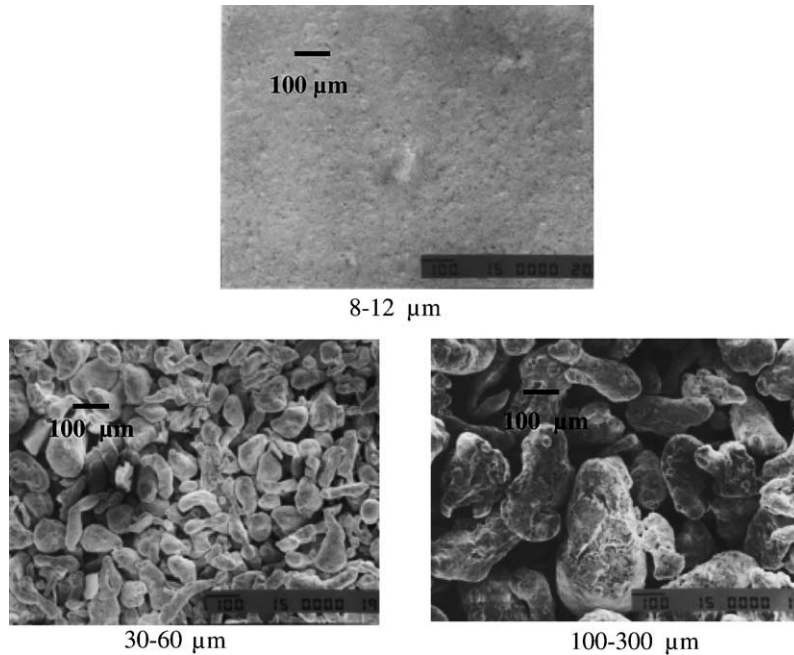


Fig. 10. SEM images of different sizes of coating particles.

Three ranges of particle size, 8–12 μm, 30–60 μm, and 100–300 μm, were employed to form microporous structures on the flat heater. The SEM images of the different particle sizes are shown in Fig. 10 with the same magnification for better visual comparison. The coating thicknesses were measured to be ≈50 μm for 8–12 μm particles, ≈150 μm for 30–60 μm particles, and ≈500 μm for 100–300 μm particles. The results shown in Fig. 11 reveal that the tested particle sizes produced similar heat transfer curves. The capillary pumping phenomenon should be stronger as the coating particle size decreases. On the other hand, fluid flow resistance for the soaked water within the microporous passageways increases as the particle size decreases. Also, the wall temperature increases due to the additional thermal resistance of conduction as the layer thickness increases for a given heat flux. Therefore, the possible enhancement from less fluid flow resistance due to larger cavity size is believed to be counterbalanced by degradation due to additional thermal resistance from conduction and less capillary pumping power.

The smallest particle size (8–12 μm) was selected to investigate the optimum coating thickness. The 8–12 μm particles are the most convenient for the coating method. Fig. 12 shows the heat transfer performance with coating thicknesses of 50, 100, 150, and 200 μm on the flat heater during tests with spray cooling and a water flow rate of 1.75 ml/min. Microporous coatings with 150 and 200 μm thicknesses showed smaller enhancement in spray heat transfer than coatings with 50 and 100 μm

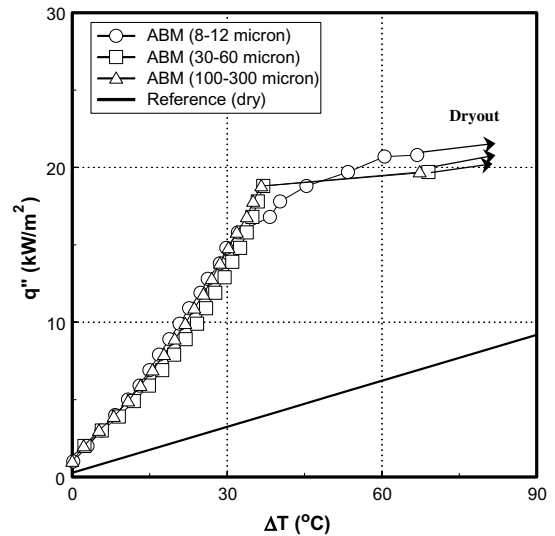


Fig. 11. Effect of microporous coating particle sizes on heat transfer performance of flat heater (water flow rate: 1.75 ml/min).

thicknesses. The 100 μm coating thickness attained the highest heat transfer coefficient among the tested thicknesses. This thickness produced up to ≈50% increase in evaporative heat transfer coefficient over the 200 μm thickness. The thicker microporous coating retains more water droplets as the coating thickness increases due to

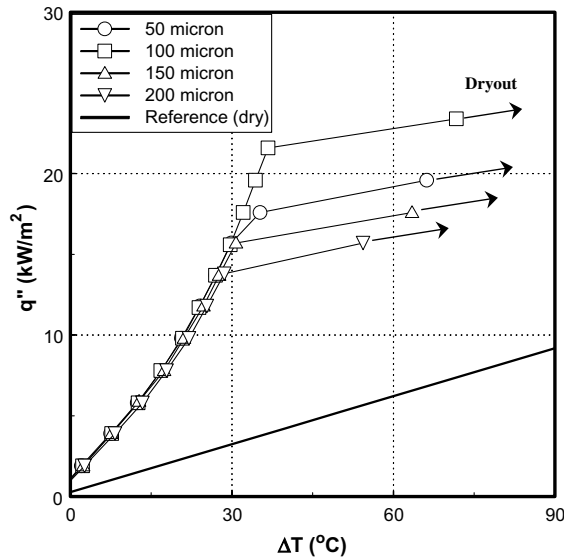


Fig. 12. Effect of microporous coating thickness on heat transfer performance of flat heater (water flow rate: 1.75 ml/min).

the larger number of microporous cavities. However, the evaporative heat transfer coefficient degrades extensively due to the additional thermal resistance to conduction as the thickness exceeds 100  $\mu\text{m}$ .

#### 4. Conclusions

Evaporative spray cooling from plain and microporous coated surfaces was investigated to understand the heat transfer performance compared to that of dry air-jet cooling. The current study investigated the effect of heater geometry (flat and cylindrical heaters) and water flow rates on spray evaporative cooling. The effects of particle sizes and coating thicknesses were also investigated.

Important findings from this study are:

- (1) Evaporative cooling with spraying water dramatically enhances the heat transfer coefficient over dry air-jet cooling due to the added heat transfer by evaporation (heat of vaporization).
- (2) The microporous coating further increases the heat transfer coefficient of evaporative spray cooling over the plain surface due to capillary pumping action. However, the heat transfer coefficient for dry air-jet cooling is unaffected by the surface microstructure.
- (3) The combination of evaporative cooling and coated microporous surface enhances the heat transfer coefficient by up to 400% relative to the reference case (dry air cooling with uncoated, plain surface).

- (4) The microporous coating extended the dryout heat flux significantly ( $\approx 21 \text{ kW/m}^2$ ) over the plain surface ( $15 \text{ kW/m}^2$ ).
- (5) Similar heat transfer improvements were observed for both flat and cylindrical heaters. The increase was less for the cylindrical than the flat heater due to the nonwetting of the surface opposite to the spray.
- (6) When heat flux is less than  $\approx 10 \text{ kW/m}^2$ , water spray amounts (1.25–2.4 ml/min) have no effect on evaporative cooling for microporous coating. However, for higher heat fluxes, the heat transfer increased with the water flow rate for both plain and microporous surfaces.
- (7) The size of coating particles has a negligible effect on heat transfer performance. A nanoporous surface is recommended for further study of particle size effect.
- (8) The 100- $\mu\text{m}$  coating thickness gave the maximum heat transfer performance.

#### Acknowledgements

This work was supported by the US Department of Energy, Office of Heavy Vehicle Technologies (OHVT) under Contract W-31-109-Eng-38. The continued support of Dr. Sid Diamond, Program Director, OHVT, is very much appreciated.

#### References

- [1] Q. Zhou, S.C. Yao, Group modeling of impacting spray dynamics, *Int. J. Heat Mass Transfer* 35 (1) (1992) 121–129.
- [2] N. Chigier, Optical imaging of sprays, *Prog. Energy Combust. Sci.* 17 (3) (1991) 211–262.
- [3] K.J. Choi, S.C. Yao, Mechanisms of film boiling heat transfer of normally impacting sprays, *Int. J. Heat Mass Transfer* 30 (1987) 311–318.
- [4] J.D. Bernardin, I. Mudawar, Film boiling heat transfer of droplet stream and sprays, *Int. J. Heat Mass Transfer* 40 (11) (1977) 2579–2593.
- [5] I. Stewart, J.J. Hagers, AISE Annual Convention and Iron & Steel Exposition, Pittsburgh, PA, 1995.
- [6] B. Horacek, J. Kim, K.T. Kiger, “Effects of noncondensable gas and subcooling on the spray cooling of an isothermal surface,” *Proceedings of ASME IMECE*, Washington, DC, 2003, IMECE 2003-41680.
- [7] R.L. Webb, *Principles of Enhanced Heat Transfer*, John Wiley and Sons, New York, 1994.
- [8] H.M. Kurihara, J.E. Myers, The effects of superheat and surface roughness on boiling coefficients, *AIChE J.* 6 (1) (1960) 83–91.
- [9] P.J. Berenson, Experiments on pool-boiling heat transfer, *Int. J. Heat Mass Transfer* 5 (1962) 985–999.
- [10] K. Nishikawa, Y. Fujita, H. Ohta, S. Hidaka, Effect of system pressure and surface roughness on nucleate boiling



- heat transfer, Mem. Fac. Eng. Kyushu Univ. 42 (2) (1982) 95–111.
- [11] S. Nishio, G.R. Chandratilleke, Steady-state pool boiling heat transfer to saturated liquid helium at atmospheric pressure, JSME Int. J., Ser.II 32 (4) (1989) 639–645.
- [12] J.P. O'Connor, S.M. You, A painting technique to enhance pool boiling heat transfer in FC-72, ASME J. Heat Transfer 117 (2) (1995) 387–393.
- [13] J.Y. Chang, S.M. You, Boiling heat transfer phenomena from micro-porous and porous surfaces in saturated FC-72, Int. J. Heat Mass Transfer 40 (18) (1997) 4437–4447.
- [14] J.Y. Chang, S.M. You, Enhanced boiling heat transfer from micro-porous surfaces: effects of a coating composition and method, Int. J. Heat Mass Transfer 40 (18) (1997) 4449–4460.
- [15] J.Y. Chang, S.M. You, Heater orientation effects on pool boiling of micro-porous-enhanced surfaces in saturated FC-72, ASME J. Heat Transfer 118 (4) (1996) 937–943.
- [16] S.J. Kline, F.A. McClintock, Describing uncertainties in single-sample experiments, ASME Mechanical Eng. 75 (1953) 3–8.
- [17] S.M. You, J.P. O'Connor, Boiling Enhancement Coating, US Patent No. 5814392, 1998.